Origin of the curved nature of Mach cone wings in complex plasmas

S. K. Zhdanov,[1] G. E. Morfill,[1] D. Samsonov,[1] M. Zuzic,[2] and O. Havnes[2]
[1]*CIPS, Max-Planck-Institut für Extraterrestrische Physik, 85740 Garching, Germany*
[2]*Department of Physics, University of Tromsø, 9037 Tromsø, Norway*
(Received 8 January 2003; revised manuscript received 16 October 2003; published 24 February 2004)

While the propagation and refraction of waves and shocks which constitute Mach cones have been well studied in continuous slowly varying stratified media such as gases, liquids, and solids, here we investigate these processes at the kinetic, discrete (or ''molecular'') level in a complex plasma where the stratification scale is of the order of the damping length. The shape of Mach cones formed by nondispersive linear sound waves in a nonuniform complex plasma was calculated analytically using the method of wave rays. The cases of transversely and longitudinally inhomogeneous media as well as a medium with a sound speed maximum were considered. The theory was compared with experimental observations of Mach cones with curved wings (dynamic Mach cones) in a two-dimensional complex plasma. A good quantitative agreement was obtained.

DOI: 10.1103/PhysRevE.69.026407 PACS number(s): 52.27.Lw

I. INTRODUCTION

Mach cones are V-shaped disturbances or shock waves produced by a supersonic object moving through a medium. While they are best known in gas dynamics [1], they also occur in solid matter [2]. Mach cones in complex (dusty) plasmas were predicted by Havnes *et al.* [3,4] and observed experimentally in a two-dimensional (2D) strongly coupled complex plasma [5–7]. They were described theoretically by Dubin [8] as a superposition of linear dispersive waves. This approach works well only in the far field, as pointed out by Ma and Bhattacharjee [9], who developed a molecular dynamics simulation of compressional and shear Mach cones. Shear Mach cones were observed experimentally by Nosenko *et al.* [10].

The interest in Mach cones in complex plasmas is high for two reasons: first, fundamental studies at the kinetic level are possible and second, it is anticipated that the cameras of the Cassini spacecraft might possibly be able to image Mach cones in Saturn's rings [3,4], when it arrives at Saturn in 2004. The dust which constitutes Saturn's rings is charged by exposure to sunlight and the Saturnian magnetospheric plasma. As a consequence, the dust orbit velocities lie in between corotational and Keplerian, depending on the particle size. The Mach cones are produced by boulders, which move in Keplerian orbits. The velocity difference between boulders and dust can be supersonic, compared to the dust acoustic speed (in the charged dust). Observation of Mach cones might therefore provide a means for remote diagnostics of complex plasmas in Saturn's rings [3,4]. They might also be used effectively for diagnosing, e.g., reactive plasmas with growing particles [11].

Complex (dusty) plasmas consist of submicron to millimeter sized particles immersed in an electron/ion plasma. The particles charge up (usually negatively) by collecting electrons and ions, and can interact with each other. Complex plasmas are characterized by a coupling constant Γ, which is the ratio of the Coulomb interaction energy and the kinetic energy of the particles. Depending on Γ, complex plasmas can be in gaseous ($\Gamma<1$), liquid ($\Gamma>1$), or crystalline ($\Gamma\gtrsim 170$) states [12].

Dusty plasmas are ubiquitous in space, e.g., interstellar and intergalactic clouds, protoplanetary disks, comet tails, and planetary rings. They are well studied in astrophysics and occur in the weakly coupled (gaseous) state [13]. The presence of the third (dust) plasma component gives rise to new wave modes, the most important being the dust acoustic wave (DAW), which was described theoretically by Rao *et al.* [14] and first observed by Barkan *et al.* [15]. The inertia in this mode is provided by charged and massive dust particles which slowly respond to electric fields thus providing oscillations of very low frequency (1–100 Hz).

The formation of plasma crystals (strongly coupled complex plasmas) was recently discovered [16–19]. This accelerated the interest in the field, and the term ''complex plasmas'' was coined. Since the macroscopic particles can be easily observed with an ordinary video camera and their arrangement is analogous to the atoms in real matter, complex plasmas can be used as a model system [20] to study phase transitions [19–23], waves [24–26], solitons [27,28], shocks [29], and Mach cones [5–7] at the kinetic level.

Complex plasmas usually consist of four components: electrons, ions, neutrals, and dust particles. The dust particles can be visualized individually, they can be strongly interacting (even forming crystal structures), and research at the most fundamental kinetic level is possible. One of the interesting questions is the identification of the range of applicability of fluid dynamics as the system is resolved to the discrete (particle) level. Complex plasmas can only be sustained by a constant input of energy to maintain ionization, making them ''open systems.'' Hence another important question concerns the thermodynamics which is applicable in this case.

Mach cones were originally considered for homogeneous and constant conditions [3,4]. The cone shows up as a straight V-shaped pattern. Measurements of the opening angle and other details of the cone, such as, for example, damping length and stand-off distance in front of the disturbing body, were suggested as a diagnostic method in planetary rings [3,30] and in dusty plasma experiments [4,31]. Mach cones in these cases are formed by DAW [14,15], which are acousticlike (weakly dispersive) waves.

In many cases the conditions in a dusty plasma may not be homogeneous and constant in time. This affects the shape of the Mach cone leading to curved patterns, so-called dynamic Mach cones (DMC). This opens up the possibility of tracing the time and/or position dependent conditions in the dusty plasma by analyzing the Mach cone pattern and its deviations from a straight V shape. In reactive experiments, where dust sizes and dust charges will change with time, the time history of the DAW velocity, which is dependent on factors such as dust mass and charge, can be reconstructed from an analysis of the DMC shape [11].

In the present paper we consider the DMC problem anew and include situations where the dusty plasma is spatially inhomogeneous. Compared to most stratified systems (e.g., the Earth's atmosphere, seismology, stratified fluids) the scale of variations occurs at the scale of particle separations (equivalent to a few or a few tens of molecular distances). Hence, by comparison with usual situations, we are in the extreme inhomogeneous limit. The Mach cone relation should be derived in this case by integrating along the wave rays, i.e., a general nonlocal problem should be solved. In the analysis, we nevertheless restrict ourselves to nondispersive dust acoustic waves and demonstrate the general ray tracing method in Sec. II. In Sec. III we reconsider the DMC method [11] for a homogeneous medium with time evolution (including fast evolution), while in Secs. IV and V we find the resulting Mach cone shapes in media which are inhomogeneous in the transverse and longitudinal directions with respect to the velocity direction of the disturbing body. The theoretical result is then compared with the experimental data.

Even though multiple Mach cones were reported [5–9], we limit ourselves to the description of the first compressional Mach cone. Since the multiple cones are usually well separated, the first cone can be treated independently.

II. WAVE RAYS

In order to analyze the shape of Mach cones we used the method of wave rays. It was developed for analysis of ship wakes [32] and used for Mach cones in Ref. [8]. We consider the propagation of wave rays through the medium and limit ourselves to nondispersive acoustic wave rays which are defined by the following set of equations:

$$\dot{\mathbf{r}}=\mathbf{v}_g, \quad \dot{\mathbf{k}}=-\partial_{\mathbf{r}}\omega, \quad \omega=kC_s, \quad \mathbf{v}_g=\mathbf{k}C_s/k. \tag{1}$$

This approach works for both compressional and shear small amplitude cones as a first approximation. The effects of dispersion are significant in the far field, where the cones disappear due to neutral gas damping.

To demonstrate all features of our approach, we first investigate the case of a spatially uniform medium where Eqs. (1) become

$$\dot{\mathbf{r}}=\mathbf{v}_g, \quad \dot{\mathbf{k}}=0, \quad \omega=kC_s, \quad \mathbf{v}_g=\mathbf{k}C_s/k, \tag{2}$$

and have a ballisticlike solution:

$$\mathbf{k}=\mathbf{k}_0=\text{const},$$

$$\mathbf{r}-\frac{\mathbf{k}}{k}C_s(t-t_0)=\mathbf{r}_0=\text{const}. \tag{3}$$

The values with 0 subscript are supposed to be known at a certain initial time $t_0<t$. As expected in a homogeneous isotropic medium, the rays are straight lines and the wave front propagates as a circle around the excitation point.

Let us assume that the wave pattern is excited by a point source which is moving with a constant velocity along a trajectory $y_{source}=0$, $x_{source}=Vt$. Since $\mathbf{r}_0$ in Eq. (3) is the starting point for any individual wave excited by the source, evidently, $\mathbf{r}_0=Vt_0\mathbf{e}_x$ should be substituted in Eq. (3) instead of $\mathbf{r}_0$. The sound ray can then be represented as

$$\begin{aligned} x-C_s(t-t_0)\cos\psi&=Vt_0,\\ y-C_s(t-t_0)\sin\psi&=0, \end{aligned} \tag{4}$$

where ψ is the angle between $\mathbf{k}$ and the x axis, and a 2D pattern is considered for simplicity.

From the mathematical point of view, Eqs. (4) are the two-parametric families of curves having the values t_0 and ψ as parameters. The envelope for these curves represents the shape of the Mach cone. The following two steps will determine the envelope. First, the parameter ψ should be eliminated. This means that the ''sound front family'' is studied instead of the ''sound ray family.'' For the problem in Eq. (3), the sound front family is simply the family of circles which are growing radially in time. We find by combining the two Eqs. (4)

$$(x-Vt_0)^2+y^2=C_s^2(t-t_0)^2. \tag{5}$$

Differentiating this relation with respect to the parameter t_0 and keeping all other values fixed gives

$$t_0=\frac{Vx-C_s^2t}{V^2-C_s^2}. \tag{6}$$

Substituting this value back into Eq. (5), we can find the relationship describing the envelope:

$$y^2=\frac{C_s^2}{V^2-C_s^2}(Vt-x)^2\equiv(Vt-x)^2\tan^2\theta, \quad x\leqslant Vt. \tag{7}$$

This is the well-known result for a classical Mach cone where θ is the opening angle of the Mach cone.

III. DYNAMIC MACH CONE

The set of Eqs. (2) can be translated to a case where the medium is homogeneous but changes with time on a time scale which is long compared to the wave period.

Let us consider a two-dimensional case. To find a solution for the dynamic problem, we make the straightforward redefinitions such that Eqs. (4) are replaced by

$$x-\cos\psi\int_{t_0}^{t}C_s(t')dt'=Vt_0,$$
$$y-\sin\psi\int_{t_0}^{t}C_s(t')dt'=0, \tag{8}$$

while Eq. (5) should be written as

$$(x-Vt_0)^2+y^2=\left(\int_{t_0}^{t}C_s(t')dt'\right)^2. \tag{9}$$

The envelope (DMC) is then defined parametrically by Eq. (9) and the first of Eqs. (8) with $\cos\psi=C_s(t_0)/V$:

$$(x-Vt_0)=\frac{C_s(t_0)}{V}\int_{t_0}^{t}C_s(t')dt'. \tag{10}$$

These relations give the general solution of the problem from which one can find the DMC profile for any given dependency $C_s=C_s(t)$. A particular case for the time-dependent sound speed $C_s=C_s(t)$ has been studied in detail in Ref. [11].

It is of interest to investigate the Mach cone profile near its origin since this region is often the only one which can be investigated experimentally. A corresponding expansion series is given by [11]

$$y^2=\frac{\alpha^2}{1-\alpha^2}(Vt-x)^2\left[1-\frac{\dot{\alpha}/\alpha}{(1-\alpha^2)^2}\frac{Vt-x}{V}+\cdots\right]. \tag{11}$$

Here, the dot denotes the derivative with respect to time, and

$$\alpha=\alpha(t)=\frac{C_s(t)}{V} \tag{12}$$

is the dynamic Mach cone. Depending on whether the sound speed increases, or decreases, in time, the Mach cone wings are bent correspondingly, as predicted in Ref. [11].

If we assume that the size of cone wings is limited by damping, and if α is small, then the expansion series is valid when the time scale τ of the sound speed variation is large enough:

$$\tau\nu\gtrsim\left(1+\frac{1}{M^2-1}\right)^{-2},\quad M=\frac{1}{\alpha}. \tag{13}$$

Here, ν is the damping rate. For the parameters listed in Ref. [11], (Eq. 13) is valid in most cases where the Mach number is large $M\gg1$.

Relation (11) gives a solution of the *direct problem*: we know that $C_s=C_s(t)$, and can obtain the cone profile from this given variation. More interesting is the inverse problem when we have experimentally measured the cone profile and want to obtain the variation of the sound speed $C_s=C_s(t)$. For this solution let us find the derivative $\partial y/\partial x$, i.e., the tangent of the opening angle θ at t_0. From Eq. (7) it follows that

$$\tan^2[\theta(t_0)]=\left(\frac{\partial y}{\partial x}\right)^2=\frac{C_s^2(t_0)}{V^2-C_s^2(t_0)}. \tag{14}$$

Equation (14) is valid along the whole cone wing, not only near the cone apex. This allows us to solve the *inverse problem* where we determine $C_s=C_s(t)$ by using the data of the curve $y=y(x,t)$ for the Mach cone at time t. A chosen point (x,y) on this curve corresponds to a wave being excited at a time t_0 at the point Vt_0, where the origin corresponds to the position of the disturbing body at time $t=0$. Another point on the Mach cone will correspond to another t_0. Since the medium is uniform in space the wave front, sent out at t_0 and arriving at (x,y) at time t will not be bent. The tangent at (x,y) will be parallel to the wave front, and the normal to the curve at the same point will cross the x axis at the point Vt_0 where the wave was excited. This gives the relation

$$Vt_0=x-\left|y(x)\left(\frac{\partial y}{\partial x}\right)\right|. \tag{15}$$

This, combined with C_s found from Eq. (14), is the solution of the inverse problem:

$$C_s(t_0)=V\frac{\left|\left(\frac{\partial y}{\partial x}\right)\right|}{\sqrt{1+\left(\frac{\partial y}{\partial x}\right)^2}}. \tag{16}$$

If we know the velocity V of the disturbing body, the time t_0 can be found and this, together with t, the observing time of the analyzed DMC, will give the time history of the velocity C_s.

Equation (16) is a solution of the general dynamic Mach cone problem with the acoustic speed varying in time and it is valid for fast variations. The Mach cone angle θ is the angle between the tangential to the cone wing and the direction of propagation, not necessarily close to the cone vertex (Fig. 1). It is remarkable that Eq. (16) depends only on the local acoustic speed, reflecting the fact that the wave rays remain straight even though the acoustic speed varies along them. In the limit of a constant acoustic speed Eq. (16) becomes the well-known Mach cone relation: $1/M=\sin(\theta)$, where θ is the angle at the cone vertex. In the limit of a slow varying acoustic speed Eq. (16) reproduces the results of Havnes *et al.* [11] [see also Eq. (11)].

IV. MACH CONE IN A TRANSVERSELY INHOMOGENEOUS MEDIUM

Waves propagating in a spatially inhomogeneous medium can be reflected if the density gradient is large enough, e.g., at a surface (total internal reflection). For gradient scales $\gg$ mean particle separation the wave rays and wave fronts are bent [33]. The reflection, or bending problem cannot be solved analytically in general. We have therefore concentrated on two particular cases: a transverse and a longitudinal

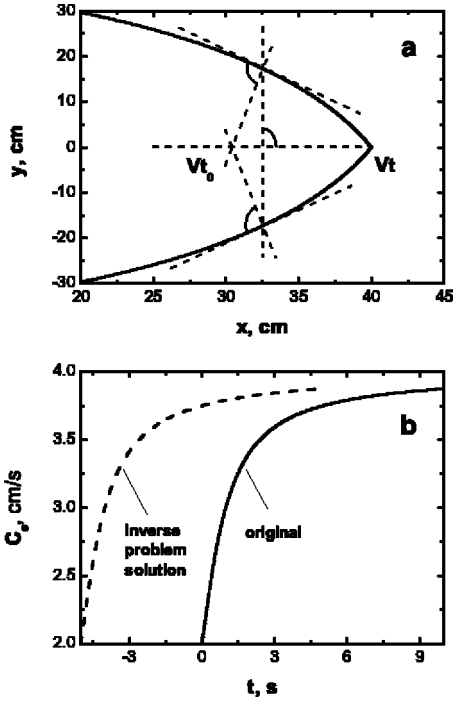

FIG. 1. Dynamic Mach cone. $C_s(t)=C_0[1+(2/\pi)\mathrm{atan}(t/\tau)]$, $C_0=2$ cm/s, $\tau=1$ s, $V=4$ cm/s. (a) For any fixed position (given by the vertically dashed line), two tangents to the cone wings can be constructed at the intersection. The perpendicular lines to these tangents cross at some point on the trajectory of the source, which excites the waves. This point corresponds to the time t_0. (b) Illustration of the inverse problem solution.

2D-inhomogeneity with respect to the velocity vector of the disturbing body. In the case of a transverse inhomogeneity, the general equations (1) are simplified, and can be written as

$$\dot{x}=\frac{k_x}{k}C_s(y),\quad \dot{y}=\frac{k_y}{k}C_s(y),\quad \dot{k}_x=0,\quad \dot{k}_y=-kC_S'(y). \tag{17}$$

This system conserves ''energy,'' where the wave frequency

$$\omega=kC_s(y)=\mathrm{const}, \tag{18}$$

which can be proved by direct differentiation. The x component of the wave vector is also conserved, $k_x=\mathrm{const}$.

For further analysis it is convenient to introduce the following parameters:

$$\beta=\frac{k_xC_0}{\omega},\quad f(y)=\left(\frac{C_0}{C_s(y)}\right)^2,$$

$$k_y=\sigma\frac{\omega}{C_0}\sqrt{f(y)-\beta^2},\quad \sigma=\pm 1, \tag{19}$$

where C_0 is a scale factor for the velocity distribution. Then the formal solution of Eqs. (17) is given by

$$C_0(t-t_0)=\int_0^y dy\,\frac{\sigma f}{\sqrt{f-\beta^2}},\quad x-Vt_0=\int_0^y\frac{\sigma\beta}{\sqrt{f-\beta^2}}. \tag{20}$$

Eliminating the parameter t_0 results in

$$x=Vt+\int_0^y dy\,\frac{\sigma\beta}{\sqrt{f-\beta^2}}-\frac{V}{C_0}\int_0^y dy\,\frac{\sigma f}{\sqrt{f-\beta^2}}. \tag{21}$$

To obtain the envelope, we have to differentiate this relationship with respect to β. This yields

$$\beta=\frac{C_0}{V},\quad x_{envelope}=Vt-\int_0^y dy\,\sigma\sqrt{\left(\frac{V}{C_s(y)}\right)^2-1}. \tag{22}$$

Equation (22) corresponds to the solution of the *direct problem*, where the sound speed distribution is known. But the *inverse problem*, the determination of the sound speed distribution from the known cone profile, can also be solved analytically. From Eq. (22) it follows that

$$C_s(y)=\frac{V\left|\frac{\partial y}{\partial x}\right|}{\sqrt{1+\left(\frac{\partial y}{\partial x}\right)^2}}. \tag{23}$$

With respect to relation (22), it is not a surprising result: during the source propagation, the cone is in a steady state, and the profile does not change in time. Note that the cone wings are bent up towards the direction of the sound speed gradient as the sound speed is increasing.

V. MACH CONE IN A LONGITUDINALLY INHOMOGENEOUS MEDIUM

In the case of a longitudinally inhomogeneous medium we have

$$\dot{x}=\frac{k_x}{k}C_s(x),\quad \dot{y}=\frac{k_y}{k}C_s(x),\quad \dot{k}_y=0,\quad \dot{k}_x=-kC_S'(x). \tag{24}$$

Here the problem is more complicated. As in Sec. IV the wave frequency is conserved along the sound rays:

$$\omega=kC_s(x)=\mathrm{const}. \tag{25}$$

The y component of the wave vector is also conserved, $k_y=\mathrm{const}$. We now introduce the following parameters, which again are similar to but not identical to those of Sec. IV:

$$\beta=\frac{k_yC_0}{\omega},\quad f(y)=\left(\frac{C_0}{C_s(x)}\right)^2,\quad k_x=\frac{\omega}{C_0}\sqrt{f(y)-\beta^2}, \tag{26}$$

where C_0 is the scale factor for the velocity distribution. The formal solution of Eqs. (24) is given by

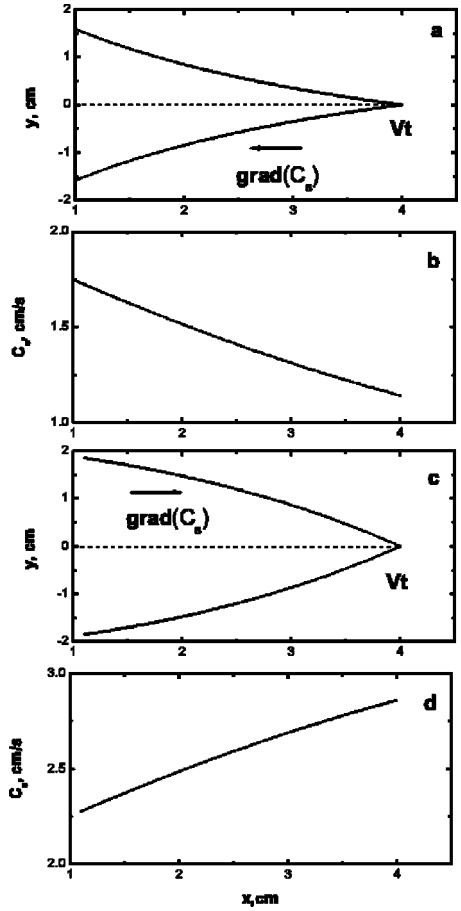

FIG. 2. Mach cone in a longitudinally inhomogeneous medium. (a,c) wing profiles; (b,d) sound speed profile. (a,b) $C_s(y)=C_0[1-(2/\pi)\mathrm{atan}(y/L)]$, (c,d) $C_s(y)=C_0[1+(2/\pi)\mathrm{atan}(y/L)]$, in both cases $C_0=2$ cm/s, $V=4$ cm/s, $L=5$ cm, $t=1$ s.

$$C_0(t-t_0)=\int_{Vt_0}^{x} dx\,\frac{f}{\sqrt{f-\beta^2}},\quad y=\int_{Vt_0}^{x} dx\,\frac{\beta}{\sqrt{f-\beta^2}}. \tag{27}$$

To find the envelope for this family of rays, one has to differentiate Eq. (27) and substitute the calculated derivatives by the relationship

$$J\equiv\frac{\partial y}{\partial\beta}\frac{\partial x}{\partial t_0}-\frac{\partial x}{\partial\beta}\frac{\partial y}{\partial t_0}=0 \tag{28}$$

(J is the Jacobian; by definition, it has to be equal to zero on an envelope).

From that we obtain

$$\beta_{envelope}=\pm\frac{C_0}{C_s(Vt_0)}\sqrt{1-\left(\frac{C_s(Vt_0)}{V}\right)^2}. \tag{29}$$

The parameter β is finally substituted back into the relations (27), and from that the envelope curve is parametrically defined:

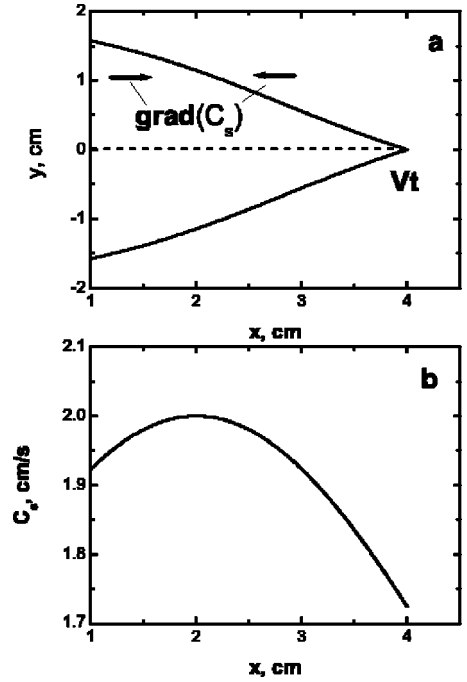

FIG. 3. Mach cone near a sound speed maximum. (a) Wing profiles; (b) sound speed profile. $C_s(y)=C_0[1+[(x-2)/L]^2]^{-1}$, $C_0=2$ cm/s, $V=4$ cm/s, $L=5$ cm, $t=1$ s.

$$C_0(t-t_0)=\int_{Vt_0}^{x} dx\,\frac{f}{\sqrt{f-\beta_{envelope}^2}},$$

$$y=\int_{Vt_0}^{x} dx\,\frac{\beta_{envelope}}{\sqrt{f-\beta_{envelope}^2}}. \tag{30}$$

The tangent of the slope angle is given by

$$\left(\frac{\partial y}{\partial x}\right)^2=\frac{C_s^2(Vt_0)+V^2[1-C_s^2(Vt_0)/C_s^2(x)]}{V^2-C_s^2(Vt_0)}. \tag{31}$$

Equations (30) and (31) describe the analytical solution of the direct problem. Some particular propagation cases are shown for illustration purposes in Fig. 2.

For instance, nearby the cone apex relation (31) becomes

$$\left(\frac{\partial y}{\partial x}\right)^2\cong\frac{C_s^2(x)}{V^2-C_s^2(x)}$$

$$\cong\frac{\alpha^2}{1-\alpha^2}\left(1-\frac{2}{1-\alpha^2}\frac{\dot{\alpha}}{\alpha}\frac{Vt-x}{V}+\cdots\right),$$

$$\alpha=\alpha(t)\equiv\frac{C_s(Vt)}{V}. \tag{32}$$

In contrast to the case of a transverse inhomogeneity discussed before, the cone is now symmetric with respect to the y axis, but not stationary. The cone profile varies in time during the propagation. Note that if the sound speed gradient is *parallel* to the direction of the moving source, the tails of the cone wings are bent towards the source trajectory be-

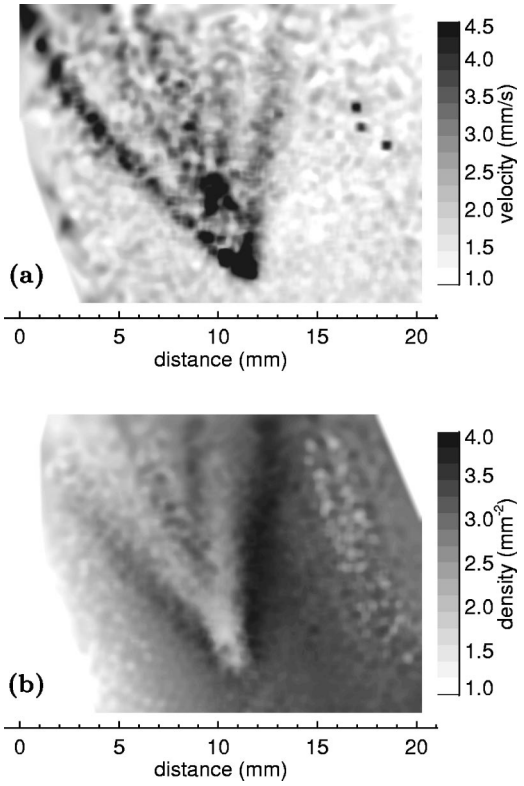

FIG. 4. Mach cone images showing particle velocity map (a) and number density map (b). The left-hand side wing is curved back. This is attributed to the lower dust-lattice speed at the edge of the lattice, where the particle number density is lower. The right-hand side wing is in the region of a constant particle number density and it is straight.

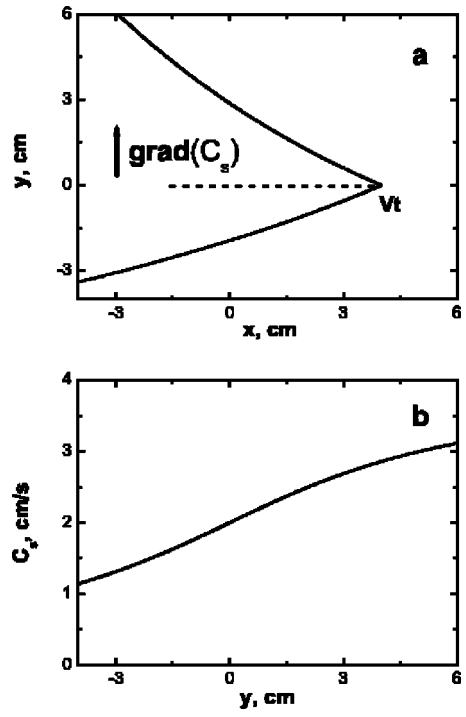

FIG. 5. Mach cone in a transversely inhomogeneous medium. (a) Wing profiles; (b) sound speed profile. $C_s(y)=C_0[1+(2/\pi)\mathrm{atan}(y/L)]$, $C_0=2$ cm/s, $V=4$ cm/s, $L=5$ cm, $t=1$ s.

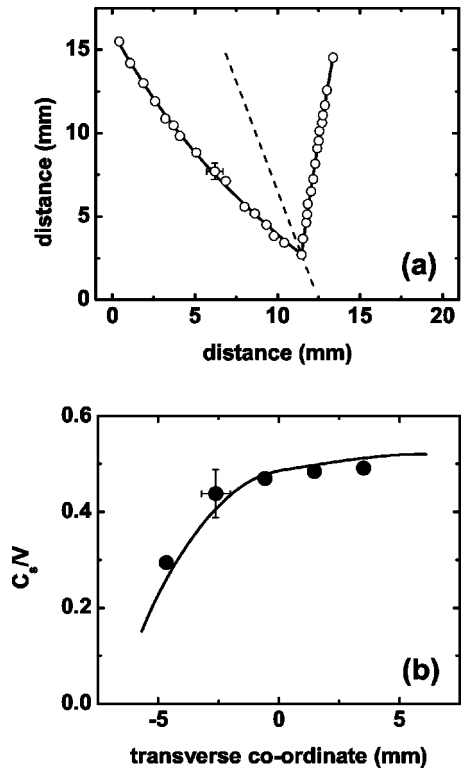

FIG. 6. (a) Shape of a Mach cone in a transversely inhomogeneous medium. The experimental data points (open circles) are taken from the velocity map [Fig. 4(a)]. Both cone wings are fitted to a third order polynomial (solid lines). The trajectory of the cone vertex is marked by a dashed line. (b) Inverse Mach number (ratio of the acoustic speed C_s to the speed of a perturbing body V) across the Mach cone trajectory. The negative direction corresponds to the left cone wing, the positive to the right. Filled circles indicate the values calculated directly from the particle number density map [Fig. 4(b)]. The solid line is calculated from the shape of the Mach cone. Typical error bars are marked on one of the data points in both plots.

cause the sound speed is faster in the front. In the opposite case the wings *bent away* from the source trajectory since the sound speed is faster behind the source. Furthermore, if the sound speed gradient changes in sign, transient forms can be observed where the cone wings have a more complicated form (see Fig. 3, where the source crosses the sound speed maximum). The inverse problem cannot then be solved analytically but it is easily solved numerically.

VI. COMPARISON WITH THE EXPERIMENT

In order to verify our theoretical results, we conducted an experiment using the setup and analysis method of Ref. [6]. The compressional Mach cones were created in a two-dimensional plasma crystal by fast particles, moving under the lattice at a constant speed. We observed Mach cones at the edge of the lattice, where the particle number density (and the dust lattice wave speed) was lower than that closer

to the center of the lattice. The dynamic Mach cone is shown in Fig. 4. Its left wing curves back [Fig. 4(a)], i.e., it has a larger opening angle close to the vertex and smaller far from it. This agrees qualitatively with the theoretical predictions for a transversely inhomogeneous medium [Fig. 5(a)]. The particle number density map is shown in Fig. 4(b). The edge of the lattice is on the left side of the field of view. The number density is lowest at the edge ($1.5\ \mathrm{mm}^{-2}$) and increases towards the center reaching a constant value of $3.3\ \mathrm{mm}^{-2}$ at 5–7 mm from the edge.

In order to reconstruct the properties of the medium using the Mach cone shape we first obtained the trajectory of the vertex [6] and fitted it to a straight line. The speed of the perturbing body was then determined to be $V=35\pm7$ mm/s. The shapes of the cone wings were then taken from the velocity map [Fig. 4(a)] and fitted with a third-order polynomial. Figure 6(a) shows the cone wings and the vertex trajectory.

Using Eq. (23) we reconstructed the acoustic speed C_s across the cone trajectory. The particle number density n across the cone trajectory was obtained from the number density map [Fig. 4(b)]. The acoustic speed is related to n (particle separation a), particle charge Q, and the Debye length λ_D by Eq. (6) in Ref. [6], which takes into account nearest neighbor interaction. Using this relationship yields values of $Q=17\,000e$ and $\lambda_D=0.34$ mm for best agreement between C_s/V obtained from the cone shape [solid line in Fig. 6(b)] and C_s/V calculated from the known density n [circles in Fig. 6(b)]. This result compares well with the values $Q=14\,000e$ and $\lambda_D=0.34$ mm reported in Ref. [6] for similar experimental conditions.

VII. DISCUSSION

We have shown theoretically and experimentally that different dusty plasma inhomogeneities can affect the Mach cone shape in different ways. The DMC therefore contains information on either the time history of changes in the medium [11] or of density gradients in the medium (or both), and its analysis should be a useful diagnostic method in dusty plasmas. However, since the effect on the DMC shape in different cases can be similar, it still remains to see if we can get unambiguous solutions if we have a combination of time changes and density changes in the medium in which the DMC is formed.

The theory developed here is based on linear nondispersive waves. A more complete theory should include nonlinearity to improve the precision in the near field (close to the cone vertex), as well as dispersion to make the far field solution more precise. Since the waves in complex plasmas (dust acoustic, compressional and transverse dust lattice) are very weakly dispersive, it is expected that the theory provides a good approximation in the far field.

Comparison with experiments showed, somewhat surprisingly, that the continuum theory developed here works reasonably well even at the discrete (kinetic) level and for strong gradients of order of a few (or a few ten's) of the elementary scales (particle separations). The theory is valid for both compressional and shear wave cones. Observations of the particle motion at the kinetic level can distinguish between the modes. In the case of excitation by a moving body, both modes are excited and since the compressional waves propagate faster, they will produce the outer cone. Weakly coupled plasmas do not support shear waves at all, of course.

[1] J. Bond, K. Watson, and J. Welch, *Atomic Theory of Gas Dynamics* (Addison-Wesley, Massachusetts, 1965).

[2] N. Cheng, Z. Zhu, C. Cheng, and M. Toksöz, Geophys. Prospect. **42**, 303 (1994).

[3] O. Havnes, T. Aslaksen, T. Hartquist, F. Li, F. Melandsø, G. Morfill, and T. Nitter, J. Geophys. Res., [Space Phys.] **100**, A1731 (1995).

[4] O. Havnes, F. Li, F. Melandsø, T. Aslaksen, T. Hartquist, G. Morfill, T. Nitter, and V. Tsytovich, J. Vac. Sci. Technol. A **14**, 525 (1996).

[5] D. Samsonov, J. Goree, Z.W. Ma, A. Bhattacharjee, H.M. Thomas, and G.E. Morfill, Phys. Rev. Lett. **83**, 3649 (1999).

[6] D. Samsonov, J. Goree, H.M. Thomas, and G.E. Morfill, Phys. Rev. E **61**, 5557 (2000).

[7] A. Melzer, S. Nunomura, D. Samsonov, Z.W. Ma, and J. Goree, Phys. Rev. E **62**, 4162 (2000).

[8] D.H.E. Dubin, Phys. Plasmas **7**, 3895 (2000).

[9] Z.W. Ma and A. Bhattacharjee, Phys. Plasmas **9**, 3349 (2002).

[10] V. Nosenko, J. Goree, Z.W. Ma, and A. Piel, Phys. Rev. Lett. **88**, 135001 (2002).

[11] O. Havnes, T.W. Hartquist, A. Brattli, G.M.W. Kroesen, and G. Morfill, Phys. Rev. E **65**, 045403(R) (2002).

[12] H. Ikezi, Phys. Fluids **29**, 1764 (1986).

[13] E. Whipple, T. Northrop, and D. Mendis, J. Geophys. Res. [Atmos.] **90**, 7405 (1985).

[14] N. Rao, P. Shukla, and M. Yu, Planet. Space Sci. **38**, 543 (1990).

[15] A. Barkan, R. Merlino, and N. D'Angelo, Phys. Plasmas **2**, 3563 (1995).

[16] H. Thomas, G. Morfill, V. Demmel, J. Goree, B. Feuerbacher, and D. Möhlmann, Phys. Rev. Lett. **73**, 652 (1994).

[17] Y. Hayashi and K. Tachibana, Jpn. J. Appl. Phys., Part 2 **33**, L804 (1994).

[18] J. Chu and I. Lin, Phys. Rev. Lett. **72**, 4009 (1994).

[19] A. Melzer, T. Trottenberg, and A. Piel, Phys. Lett. A **191**, 301 (1994).

[20] H. Thomas and G. Morfill, Nature (London) **379**, 806 (1996).

[21] H. Thomas and G. Morfill, J. Vac. Sci. Technol. A **14**, 501 (1996).

[22] A. Melzer, A. Homann, and A. Piel, Phys. Rev. E **53**, 2757 (1996).

[23] J. Pieper, J. Goree, and R. Quinn, Phys. Rev. E **54**, 5636 (1996).

[24] F. Melandsø, Phys. Plasmas **3**, 3890 (1996).

[25] M. Zuzic, H. Thomas, and G. Morfill, J. Vac. Sci. Technol. A **14**, 496 (1996).

[26] A. Homann, A. Melzer, R. Madani, and A. Piel, Phys. Lett. A **173**, 242 (1998).
[27] D. Samsonov, A. Ivlev, R. Quinn, G. Morfill, and S. Zhdanov, Phys. Rev. Lett. **88**, 095004 (2002).
[28] S.K. Zhdanov, D. Samsonov, and G.E. Morfill, Phys. Rev. E **66**, 026411 (2002).
[29] D. Samsonov, G. Morfill, H. Thomas, T. Hagl, H. Rothermel, V. Fortov, A. Lipaev, V. Molotkov, A. Nefedov, O. Petrov, A. Ivanov, and S. Krikalev, Phys. Rev. E **67**, 036404 (2003).
[30] A. Brattli, O. Havnes, and F. Melandsø, J. Plasma Phys. **9**, 958 (2002).
[31] O. Havnes, F. Li, T. Hartquist, T. Aslaksen, and A. Brattli, Planet. Space Sci. **49**, 223 (2001).
[32] G. Crapper, *Introduction to Water Waves* (Horwood, Chichester, 1984).
[33] L. Landau and E. Lifshitz, *Hydrodynamics* (Nauka, Moscow, 1988).